

Research Article

Tenascin-X in amniotic fluid and reproductive tissues of pregnancies complicated by infection and preterm prelabor rupture of membranes[†]

Kara M. Rood ^{1,*}, Catalin S. Buhimschi^{1,2}, Guomao Zhao³, Emily A. Oliver¹, Taryn Summerfield¹, Mert Ozan Bahtiyar⁴ and Irina A. Buhimschi^{2,3}

¹Department of Obstetrics & Gynecology, The Ohio State University College of Medicine, Columbus, Ohio, USA; ²Department of Pediatrics, The Ohio State University College of Medicine, Columbus, Ohio, USA; ³Center for Perinatal Research, The Research Institute at Nationwide Children's Hospital, Columbus, Ohio, USA and ⁴Department of Obstetrics, Gynecology & Reproductive Sciences, Division of Maternal-Fetal Medicine, Yale School of Medicine, New Haven, Connecticut, USA

***Correspondence:** Department of Obstetrics and Gynecology, 395 West 12th Avenue, The Ohio State University, Columbus, Ohio 43210, USA. E-mail: kara.rood@osumc.edu

[†]**Grant support:** This project was supported by National Institutes of Health/Eunice Kennedy Shriver National Institute of Child Health and Human Development (NIH/NICHD) R01HD062007-01A1 to CSB and IAB, by The Research Institute, Center for Perinatal Research, at Nationwide Children's Hospital, Columbus, Ohio, and by Maternal Fetal Medicine Division of Department of Obstetrics, Gynecology & Reproductive Sciences of Yale University, New Haven, Connecticut. Edited by Dr. Romana Nowak, PhD, University of Illinois Urbana-Champaign

Received 18 July 2018; Revised 5 September 2018; Accepted 30 September 2018

Abstract

Preterm prelabor rupture of membranes (PPROM), which can precede or follow intra-amniotic infection/inflammation (IAI), is a poorly understood pregnancy complication. Tenascin-X (TNX) is a connective tissue extracellular matrix protein that regulates fibrillogenesis of collagens I, III, and V. Our goal was to investigate the presence and level of soluble TNX (sTNX) in amniotic fluid (AF) and TNX expression in reproductive tissues of pregnancies complicated by PPRM and IAI. We prospectively recruited 334 women pregnant with singletons who had a clinically indicated amniocentesis for genetic karyotyping, lung maturity testing, or rule-out IAI in the presence or absence of PPRM. We quantified TNX expression in fetal membranes, myometrium, cervix, and placenta using immunological methods and qRT-PCR. In pregnancies with normal outcomes, AF sTNX levels were GA-regulated with lower levels toward term. IAI significantly upregulated AF sTNX levels independent of membrane status. AF sTNX levels inversely correlated with fetal membranes tenascin XB (*TNXB*) mRNA level, which was significantly downregulated by IAI. Western blotting identified characteristic ~75 and ~140 kDa sTNX forms in both AF and fetal membranes. Fetal membranes, placenta, and cervix constitutively express TNX with the highest abundance in the amnion. Amnion TNX richness is significantly lost in the setting of IAI. Our results suggest that fetal membranes may be a source of AF sTNX whereby protein and mRNA expression seem to be significantly impacted by inflammation independent of fetal membrane status. A more thorough understanding of TNX changes may be valuable for understanding spontaneous PPRM and to potentially develop therapeutic targets.

Summary Sentence

Fetal membranes may be a source of amniotic fluid soluble tenascin-X, with both protein and mRNA levels significantly affected by inflammation independent of fetal membrane status.

Key words: pregnancy, infection, collagen, fetal membranes, labor.

Abbreviations

TNX:	Tenascin-X
TNXB :	Tenascin XB
sTNX:	Soluble TNX
AF:	Amniotic fluid
PPROM:	Preterm prelabor rupture of the membranes
ECM:	Extracellular matrix
EDS:	Ehlers-Danlos Syndrome
IAI:	Intra-amniotic infection
GA:	Gestational age
YNHH:	Yale New Haven Hospital
IQR:	Interquartile range
LDH:	Lactate dehydrogenase
HCA:	Histologic chorioamnionitis

Introduction

Preterm prelabor rupture of the membranes (PPROM) affects 3–4% of all pregnancies and precedes 40–50% of all preterm births [1]. There are multiple etiologies of PPRM; however, based on traditional microbiological culture results, approximately 30–45% of PPRM cases are associated with intra-amniotic infection (IAI), although it is unclear whether infection is a cause or consequence of PPRM [2,3]. There are many theories regarding the actual pathophysiology of PPRM, indicating the etiology is complex and likely multifactorial [4–7]. Interestingly, connective-tissue disorders are associated with weakened fetal membranes and an increased incidence of PPRM [8].

Fetal membranes, comprised of the amnion and the chorion, form the innermost layer of the intra-amniotic cavity [9]. They are connected by extracellular matrix (ECM) and provide structural integrity to the intrauterine cavity [10,11]. ECM, which is comprised of fibrous proteins along with various types of collagen, provides the architectural and structural framework of the fetal membranes [10,12]. Degradation of the collagen-rich ECM connecting the amnion and chorion layers of the fetal membranes is one of the key events leading to rupture of membranes [13,14].

Tenascins are a family of ECM glycoproteins with roles in collagen deposition and assembly, resistance to proteolysis, modulation of collagen stiffness, and cell signaling [15,16]. Tenascin-X (TNX) plays important roles in organizing and maintaining the structure of tissues that support the body's muscles, joints, organs, and skin (connective tissues), organizing and stabilizing elastic fibers that provide flexibility and elasticity to connective tissues, and production and assembly of certain types of collagen that strengthen and support connective tissues throughout the body [17–20].

TNX is the only tenascin described so far to exert a crucial architectural function; its deficiency has been directly linked with Ehlers-Danlos Syndrome (EDS), a heritable connective tissue disorder known to be associated with fibrillar collagen defects [21]. Individuals with EDS show clinical symptoms consistent with ECM structural defects including skin and joint laxity, vascular fragility, and poor wound healing [22]. During pregnancy, EDS has been

associated with pelvic instability, postpartum hemorrhage, preterm birth, and PPRM [23,24]. For example, Barabas and colleagues showed that 72% of EDS patients were delivered prematurely after PPRM [25]. Based on the above evidence, it is plausible that TNX could be an active participant in PPRM. Here we sought to evaluate the presence and levels of soluble TNX (sTNX) in amniotic fluid (AF) and TNX expression in reproductive tissues of pregnancies complicated by PPRM and IAI.

Materials and methods

Patients and amniotic fluid collection

A consortium diagram displaying the distribution of samples in our study is presented in Supplementary Figure S1. Using a cohort study design, we investigated AF samples from 334 women pregnant with singletons who had a clinically indicated amniocentesis for the purpose of second trimester genetic karyotyping (GA, median [interquartile range (IQR)]: 19 [17–20] weeks, n = 34); third trimester fetal lung maturity testing (GA: 36 [35–37] weeks, n = 31), or to rule-out IAI in women who had preterm labor contractions refractory to tocolysis, PPRM, or advanced cervical dilatation (≥ 3 cm) (GA: 27 [24–31] weeks, n = 269). Out of the last group, 226 women delivered preterm in the setting of Yes-IAI intact membranes (n = 64), Yes-IAI PPRM (n = 50), No-IAI intact membranes (n = 64), and No-IAI PPRM (n = 48). Forty-three women had No-IAI intact membranes and delivered at term (> 37 weeks).

GA was determined based on last menstrual period confirmed by an ultrasound examination prior to 20 weeks [26]. Preterm labor was defined as documented cervical effacement and/or dilatation in patients < 37 weeks of gestation with the presence of regular uterine contractions [27]. PPRM was confirmed by an amniocentesis-dye positive test or collection of vaginal AF that was positive for “pooling,” “nitrazine,” or “ferning” [28]. Idiopathic preterm birth was established on women who delivered < 37 weeks in the absence of IAI and histologic chorioamnionitis (HCA) [6]. Inclusion criteria were singleton non-anomalous gestation between 24 weeks 0 days and 33 weeks and 6 days, who presented with advanced cervical dilatation (≥ 3 cm), bulging membranes, persistent and painful uterine contractions unrelieved by hydration or tocolysis, or fever ($\geq 38^\circ\text{C}/100.4^\circ\text{F}$). Exclusion criteria were presence of viral hepatitis infection, human immunodeficiency virus, multiple gestations, anhydramnios, abnormal karyotype, or congenital anomalies. All women were recruited at Yale New Haven Hospital (YNHH), provided written informed consent, and were followed prospectively until delivery. The Human Investigation Committee of Yale University approved the study protocol.

Chemical and microbiological studies of the amniotic fluid

Following retrieval under sterile conditions by trans-abdominal amniocentesis, AF was analyzed by the YNHH clinical and microbiological laboratories for glucose concentration, white blood cell count, lactate dehydrogenase (LDH) activity, Gram staining, and

culturing for aerobic and anaerobic bacteria including *Ureaplasma* and *Mycoplasma* species. Results were available to the clinical team for management of the case; final cultures were reported 5 days after culturing. AF glucose cut-off ≤ 15 mg/dL, LDH level ≥ 419 U/L, positive Gram stain, and/or culture result were considered suggestive of IAI [29]. Presumptive identification of infection was based on standard microbiological criteria of colony morphology, medium reaction, Gram stain, and the use of a VITEK 2 automated card system (bioMérieux, Hazelwood, MO, <http://www.biomerieux-usa.com>). The remaining AF was transported to the research laboratory, spun at 3000 g at 4°C for 20 min, aliquoted in polypropylene cryotubes, and stored at -80°C until analysis.

Biological samples

Following enrollment, maternal blood was retrieved for all cases by sterile venipuncture. Per study design, AF was available for analysis in all cases. Within minutes from delivery of the placenta, a full thickness biopsy was retrieved in sterile fashion from the central portion of the placenta. Approximately half of the tissue biopsy was fixed in formalin. For the second half, decidua basalis was dissected from the villous trophoblast, rinsed in sterile saline, frozen in liquid nitrogen, and kept at -80°C for RNA studies. A full thickness biopsy of the fetal membranes was also retrieved, fixed in formalin or frozen similar to the placental tissues.

As tissue control, we used cervix ($n = 3$) retrieved from women who had a hysterectomy for morbidly adherent placenta. Myometrial tissues were obtained from a group of healthy, term, nonlaboring women ($n = 5$, GA: 38–40 weeks) undergoing scheduled elective Cesarean delivery for indications such as fetal malpresentation or prior Cesarean delivery. All term cases had reassuring fetal heart rate patterns prior to surgery. Both cervix and myometrium were placed in formalin and fixed in paraffin prior to immunohistochemistry.

Placental evaluation for histologic chorioamnionitis

In all preterm birth cases, hematoxylin and eosin stained sections of extraplacental membranes (amnion and chorio-decidua), chorionic plate, chorio-decidua, and umbilical cord were examined systematically for inflammation. Three stages of HCA (stage I: intervillitis, stage II: chorionic inflammation, and stage III: full-thickness inflammation of both chorion and amnion) were complemented by a previously described histological grading system that includes four grades of inflammation of the amnion, chorio-decidua, and umbilical cord [30]. Maternal HCA was defined as absent (amnionitis grade 0 = 0), mild (amnionitis grades 1–2 = 1), or severe (amnionitis grades 3–4 = 2) [31]. A similar scoring system was used for fetal HCA: absent (chorionic plate 0 and funisitis 0 = 0), mild (chorionic plate I–II and funisitis grades 1–2), or severe (chorionic plate III and funisitis grades 3–4).

Enzyme-linked immunosorbent assays of human amniotic fluid soluble tenascin-X

Soluble TNX (Kamiya Biomedical Company, Seattle, WA) immunoassays were performed in duplicate, according to the manufacturer's instructions by investigators unaware of the clinical presentation or outcome. The minimal detectable concentration for TNX was 1 ng/mL.

Western blotting for tenascin-X

AF samples, fetal membranes lysate, and maternal serum of patients enrolled preterm with and without IAI and PPRM were investigated for presence and forms of sTNX. Western blotting was performed on 4–20% SDS-PAGE gels (Bio-Rad Laboratories, Hercules, CA) under reducing conditions. Gels were loaded with equal amount of total protein. After electrophoretic transfer, polyvinylidene difluoride membranes were blocked with 5% milk, and then incubated overnight at 4°C with sheep polyclonal anti-Tenascin X antibody (R&D Systems, 1:200, Minneapolis, MN, Supplementary Table S1). Detection was performed using horseradish peroxidase-linked secondary antibody and chemiluminescence (ECL-Plus, Amersham Biosystems).

N-linked de-glycosylation was carried out using N-glycosidase F, α -2-3,6,8,9-neuraminidase, and endo- α -N-acetyl-galactosaminidase as previously described [32]. This was done under reducing conditions with β -mercaptoethanol according to the manufacturer's instructions (Calbiochem-EMD Chemicals Inc., Gibbstown, NJ).

Tenascin-X immunohistochemistry and immunofluorescence

Tissues were available for all patient groups included in this analysis. TNX tissue presence and level of expression were investigated by immunohistochemistry in the following groups of 55 samples: fetal membranes ($n = 4$, Yes-IAI intact membranes; $n = 5$, Yes-IAI PPRM; $n = 4$, No-IAI intact membranes; $n = 4$, No-IAI PPRM; $n = 5$, term non-labor), placenta ($n = 8$), cervix ($n = 5$), and myometrium ($n = 20$). Paraffin sections (5 μ m) were deparaffinized in xylene and rehydrated with graded ethanol to potassium phosphate-buffered saline solution, pH 7.2. Following antigen retrieval with 10 mM citrate buffer (pH = 5.5), the sections were pretreated with 1.5% hydrogen peroxide for 15 min followed by 1-h blocking in 5% donkey serum. The sections were then incubated overnight at 4°C with sheep polyclonal anti-TNX antibody (R&D Systems, 1:50 dilution). Detection was performed with biotinylated donkey anti-sheep IgG (Jackson ImmunoResearch, West Grove, PA, 1:600 dilution) followed by avidin-biotin complex incubation and NovaRed substrate exposure (Vectastain Elite ABC, Vector Laboratories, Burlingame, CA). Specificity of staining was confirmed by omitting the primary antibodies. Specific TNX staining in the amnion was evaluated semi-quantitatively in a blinded fashion from three random fields per slide. Staining intensity was scored on a scale from 0 (absent) to 5 (intense).

Double immunofluorescence was performed on select tissues to co-localize TNX immunoreactivity relative to infiltrating immune cells which were detected by expression of the pan-leukocyte marker CD45 [33]. After deparaffinization and antigen retrieval with citrate buffer, the slides were blocked with 100 mM glycine for 20 min followed by 10% donkey serum for 1 h at room temperature. Slides were further incubated overnight at 4°C with the cocktail of primary antibodies anti-TNX (1:50, R&D Systems) and anti-CD45 (1:500, Abcam, Cambridge, MA). Following washing, slides were exposed for 1 h at room temperature to secondary antibody cocktail contained 2 μ g/mL of donkey anti-sheep IgG conjugated to Alexa Fluor 488 and 2 μ g/mL of donkey anti-rabbit IgG conjugated to Alexa Fluor 594 plus 1 μ g/mL DAPI. Slides were mounted with ProLong Gold Antifade medium and images captured using a Zeiss fluorescent microscope (Zeiss, Thornwood, NY).

Table 1. Demographic, clinical, laboratory, and outcome characteristics of women with symptoms of preterm birth that provided amniotic fluid samples for tenascin-X levels (n = 269).

Variable	Rule-out infection amniocenteses					P value
	No-IAI ^a Intact & TB n = 43	No-IAI ^a Intact & PTB n = 64	No-IAI ^a PPROM & PTB n = 48	Yes-IAI ^a PPROM & PTB n = 50	Yes-IAI ^a Intact & PTB n = 64	
<i>Clinical and outcome characteristics at amniocentesis and at delivery</i>						
Maternal age, years ^b	24 [20–31]	27 [20–32]	28 [24–34]	30 [25–34]	25 [21–33]	0.002
Parity ^b	0 [0–1]	0 [0–1]	0 [0–1]	1 [0–2]	1 [0–1]	0.101
Gravidity ^b	2 [1–3]	2 [1–4]	2 [1–3]	3 [2–5]	3 [1–3]	0.342
History of preterm birth ^c	7 (16)	19 (30)	12 (25)	13 (26)	15 (23)	0.487
GA at amniocentesis, weeks ^b	27 [24–32]	26 [22–30]	32 [29–33]	27 [24–30]	25 [23–27]	<0.001
GA at delivery, weeks ^b	39 [38–39]	30 [25–33]	33 [31–33]	27 [25–30]	25 [23–27]	<0.001
Amniocentesis-delivery interval, days ^b	72 [51–95]	9 [3–27]	2 [1–8]	0 [0–1]	0 [0–0]	<0.001
Amniocentesis-delivery interval < 7 days ^c	0 (0)	30 (47)	37 (75)	48 (96)	55 (86)	<0.001
Birthweight, grams ^b	3280 [2929–3598]	1470 [912–2001]	1870 [1534–2148]	1030 [770–1479]	830 [660–1120]	<0.001
<i>Amniotic fluid laboratory test results</i>						
Glucose, mg/dL ^b	34 [25–45]	32 [21–40]	28 [21–40]	4 [2–11]	2 [2–7]	<0.001
LDH activity, U/L ^b	157 [106–198]	161 [124–253]	140 [105–204]	747 [531–1988]	969 [580–2235]	<0.001
WBC count, cells/mm ³ ^b	4 [0–10]	3 [1–8]	8 [2–22]	1000 [159–2973]	730 [213–1740]	<0.001
Positive Gram stain ^c	0 (0)	0 (0)	0 (0)	28 (56)	45 (70)	<0.001
Positive culture results ^c	0 (0)	0 (0)	0 (0)	43 (86)	49 (86)	<0.001
<i>Placental histology results</i>						
	n = 8	n = 50	n = 45	n = 49	n = 57	
Chorionic plate inflammation, stage ^b	0 [0–1]	0 [0–1]	0 [0–0]	3 [2–3]	3 [3–3]	<0.001
Amnionitis, grade ^b	0 [0–0]	0 [0–0]	0 [0–0]	3 [2–4]	3 [2–4]	<0.001
Chorio-decidualitis, grade ^b	0 [0–1]	1 [1–3]	0 [0–1]	3 [3–4]	3 [3–4]	<0.001
Funisitis, grade ^b	0 [0–0]	0 [0–0]	0 [0–0]	3 [0–4]	2 [0–4]	<0.001

^aIAI was defined by Mass Restricted score 3 or 4, indicative of severe intra-amniotic inflammation.

^bData presented as median (interquartile range) and analyzed by Kruskal-Wallis ANOVA on ranks.

^cData presented as n (%) and analyzed by the chi-squared test.

Abbreviations: IAI, intra-amniotic inflammation; WBC, white blood cells; PTB, preterm birth < 37 weeks; TB, term birth > 37 weeks; GA, gestational age; LDH, lactate dehydrogenase.

Quantitative RT-PCR procedures and primer sequences

Total RNA was isolated using TRIzol[®] Reagent (Invitrogen Life Technologies, Carlsbad, CA) with homogenization followed by chloroform separation, isopropanol precipitation, and rehydration with nuclease free water. Reverse transcription was carried out with Superscript[®] II Reverse Transcriptase (Invitrogen Life Technologies) using oligo (deoxythymidine) primers to synthesize first strand complementary DNA (cDNA). The following TaqMan Gene Expression Assays (Applied Biosystems, Foster City, CA) were used for qRT-PCR: Hs00372889_g1 for tenascin XB (*TNXB*), and housekeeping genes: Hs00265497_m1 (ribosomal protein L30, *RPL30*) and Hs99999907_m1 (beta-2-microglobulin, *B2M*). Each 20 μ L reaction consisted of 1 μ L cDNA (500 ng), 1 μ L TaqMan Gene Expression Assay, 10 μ L TaqMan Fast Advanced Master Mix, and 8 μ L of nuclease free water. Amplifications were performed on the StepOnePlus Real-Time PCR System (Applied Biosystems).

Statistical analysis

Statistical analyses were performed with Sigma Stat, version 2.03 (SPSS Inc., Chicago, IL) and MedCalc (Broekstraat, Belgium) statistical software. Normality testing was performed using the Shapiro-Wilk test. Data were compared with Mann-Whitney rank sum test, one-way ANOVA followed by Holm-Sidak tests (parametric) or Kruskal-Wallis ANOVA on ranks followed by Dunn's test (non-parametric), or two-way ANOVA as appropriate. Statistical analysis of the immunoassay data was performed after logarithmic transformation. Spearman correlations were used to measure co-linearity

between the selected independent variables. Comparisons between proportions were done with chi-squared tests. $P < 0.05$ was considered significant throughout the analysis.

Results

Clinical and laboratory characteristics of the study population

Demographic and outcome characteristics of the women at amniocentesis are presented in Supplementary Table S2. Women who had a genetic amniocentesis were older and recruited at an earlier GA compared to the other two groups. By study design women who had an amniocentesis to rule-out infection more often had uterine contractions, advanced cervical dilatation, PPROM, and signs and symptoms of clinical chorioamnionitis.

The clinical, laboratory, and outcome characteristics for the "rule-out infection" group were analyzed separately and are presented in Table 1. Women with Yes-IAI and intact membranes that delivered preterm were delivered at earlier GA and more often delivered a baby of lower birthweight. The results of the chemical and microbiological studies of the AF showed that women with Yes-IAI had higher AF LDH levels and white blood cell counts, and lower AF glucose levels, independent of PPROM. They also had higher frequencies of positive microbial culture and Gram stain. Histological examination of fetal membranes, chorionic plate, and chorio-decidua demonstrated significantly higher grades of histological inflammation in the group of women with Yes-IAI.

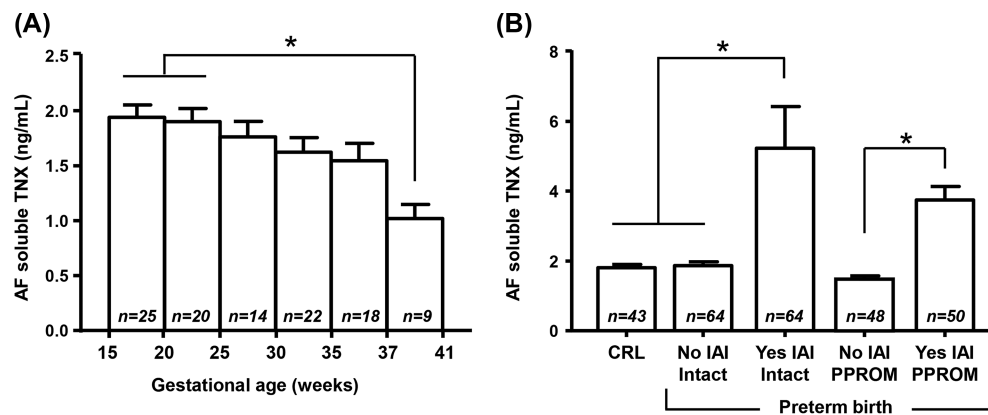


Figure 1. (A) Amniotic fluid (AF) mean soluble tenascin-X (sTNX) levels and standard error mean detected in women who had a normal pregnancy outcome (second trimester genetic amniocentesis $n = 34$, second trimester rule-out infection that delivered at term $n = 43$, and third trimester lung maturity women $n = 31$). (B) AF mean sTNX levels and standard error mean detected in women who had an amniocentesis to rule-out intra-amniotic fluid infection/inflammation (IAI) in the setting of intact or preterm prelabor rupture of membranes (PPROM). Samples included in this analysis were from women who delivered preterm. Within each graph, * denotes statistical significance at $P < 0.05$.

Gestational age regulation of soluble tenascin-X in human amniotic fluid

First, we analyzed whether AF sTNX levels exhibit GA regulation in the absence of IAI. We limited our analysis to AF from women with normal pregnancy outcome. This included women who had an amniocentesis for either genetic amniocentesis ($n = 34$), rule-out infection and ultimately delivered at term ($n = 43$), or lung maturity ($n = 31$) purposes. We found that AF sTNX concentration varied across human gestation, with significant decrease in sTNX levels approaching term ($r = 0.55$, $P = 0.002$, Figure 1A).

Soluble tenascin-X levels in the amniotic fluid of women with intra-amniotic inflammation and preterm birth

We analyzed AF samples retrieved from women with signs or symptoms of preterm birth who had an amniocentesis to rule-out infection. Cases were grouped by membrane status and IAI severity. We determined that women with Yes-IAI had significantly increased AF sTNX ($P < 0.001$, Figure 1B). These findings were upheld after correction for GA and membrane status, implying that IAI upregulated AF sTNX independent of membrane status ($P < 0.001$).

To further validate the ELISA findings and to investigate the proteoforms underlying TNX immunoreactivity, we performed western blots on TNX. As shown in Figure 2A, the anti-TNX antibody detected in maternal serum bands spanning from ~ 75 and ~ 140 kDa (marked by arrowheads), which correspond to the expected size of monomeric C-terminal fragments of TNX (lanes 1–2) [34]. Next, we examined fetal membranes of women who delivered preterm in the presence or absence of IAI (Figure 2B). Fetal membranes lysate displayed the characteristic ~ 75 and ~ 140 kDa TNX bands independent of infection (lanes 5–8). In IAI, the ~ 140 kDa TNX band was diminished in its intensity with predominance of the ~ 75 kDa TNX band.

In contrast to maternal serum and the fetal membranes lysate, AF displayed a more complex TNX band pattern (lanes 9–16, Figure 2C). In addition to the characteristic ~ 75 and ~ 140 kDa forms, we found additional TNX immunoreactive bands at ~ 30 to ~ 64 kDa, independent of IAI or status of the membranes. However,

in some IAI AF samples of women with intact membranes (lane 13) or PPROM (lane 16), the ~ 140 kDa and ~ 75 kDa TNX bands were absent. In these cases, TNX species of lower molecular weights between ~ 10 and ~ 64 kDa were observed. Deglycosylation experiments (lanes 17–20, Figure 2D) suggested that the TNX proteoforms detected in the 75–140 kDa region were glycosylated, as observed by the shift to lower molecular weights.

Expression level of tenascin-X in fetal membranes, myometrium, cervix, and placenta

In Figure 3A, we displayed the *TNXB* mRNA expression level in fetal membranes among our four study groups. In contrast to AF, *TNXB* mRNA expression in Yes-IAI was significantly downregulated independent of membrane status (two-way ANOVA, IAI $P < 0.001$, PPROM $P = 0.570$). We found an inverse correlation between *TNXB* mRNA expression in fetal membranes and AF TNX levels ($r = -0.787$, $P < 0.001$, Figure 3B) in women with Yes-IAI. Fetal membranes, myometrium, cervix, and placental tissues expressed TNX (Figure 3C). However, fetal membranes had the greatest *TNXB* mRNA expression (one-way ANOVA, $P = 0.006$), which may be due to its abundance of collagen.

Immunostaining of tenascin-X

By immunohistochemistry we found that TNX was localized in fetal membranes, myometrium, cervix, and placenta, albeit fetal membranes and myometrium stained more intensely (Figure 4). Negative control slides with the primary antibody omitted were devoid of staining (not shown).

The amnion layer (black arrow), providing tensile strength to the fetal membranes, and choriodecidua displayed strong TNX immunoreactivity in the absence (Figure 5A), but not in the presence of HCA in the setting of IAI (Figure 5B). At high magnification (Figure 5C and D), TNX was highly abundant in the cytoplasm of amnion cells in the absence of inflammation, but absent in gestations complicated by infection. Furthermore, in fetal membranes with infection we observed that the inflammatory cells invading choriodecidua, marked by green fluorescent arrowheads (Figure 5D, insert), were surrounded by a clear zone, which may suggest that in Yes-IAI TNX might be degraded together with the ECM. Semiquantitative

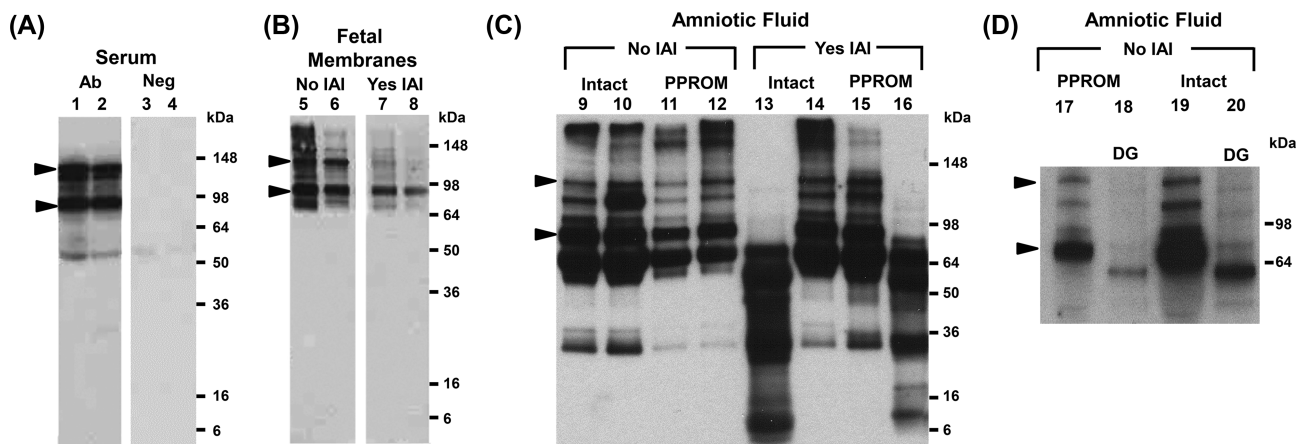


Figure 2. (A) Representative western blots demonstrating immunoreactive proteoforms of soluble tenascin-X (sTNX) in human serum (lanes 1 and 2) of two women who delivered preterm in the setting of intra-amniotic fluid infection (IAI) and histologic chorioamnionitis. As shown, serum displays TNX immunoreactivity at ~75 and ~140 kDa (marked by arrowheads). Negative controls are presented on lanes 3 and 4 where primary antibody was substituted with nonimmune serum. (B) Fetal membranes TNX forms were identified at ~75 and ~140 kDa, in a similar fashion to serum and AF (lanes 5–8). (C) Representative western blots of amniotic fluid retrieved from women without (No) or with (Yes) IAI in the setting of either intact or preterm prelabor rupture of membranes (PPROM) (lanes 9–16). In the absence of IAI, the characteristic TNX bands at ~75 and ~140 kDa were identified. In several AF samples of women with IAI, the characteristic ~140 kDa sTNX band was absent independent of membrane status (lanes 13 and 16). In these cases, sTNX species of lower molecular weights were identified. (D) Deglycosylation (DG) of two AF samples (lanes 17 and 19) showed that the sTNX proteoforms were glycosylated, given the shift to a lower molecular weight (lanes 18 and 20).

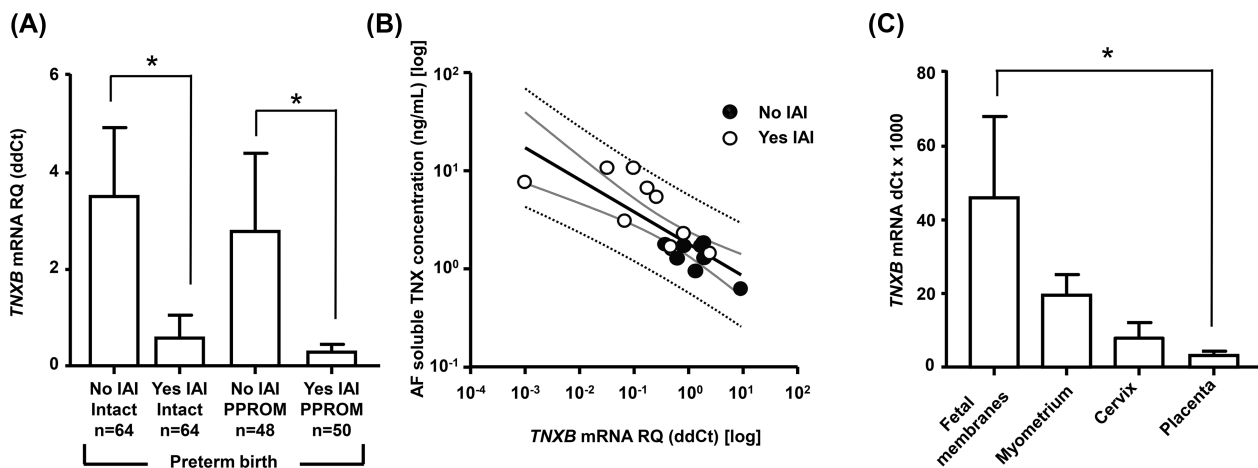


Figure 3. (A) Mean tenascin XB (*TNXB*) and standard error mean mRNA levels in the fetal membranes of women with (Yes) and without (No) intra-amniotic fluid infection/inflammation (IAI) in the setting of either intact or preterm prelabor rupture of membranes (PPROM). (B) Relationship between amniotic fluid (AF) soluble tenascin-X (TNX) levels and *TNXB* mRNA levels in women with IAI. Thick black line, linear regression line; thick gray lines, 95% confidence intervals; dotted black lines, 95% prediction intervals. (C) Mean *TNXB* and standard error mean mRNA levels in reproductive tissues (fetal membranes, myometrium, cervix, and placenta). In panel C, the thick line represents the median and graph bars display the interquartile range. Within each graph, * denotes statistical significance at $P < 0.05$.

analysis of the histological slides demonstrated that amnion TNX staining intensity did not significantly vary with status of the membrane (Figure 5E, two-way ANOVA, $P = 0.557$), but did with presence of infection ($P < 0.001$). In pregnancies complicated by IAI, fetal membranes double immunostaining for TNX and CD45 confirmed the cells infiltrating the tissues are leukocytes (Figure 5F). These inflammatory cells did not express TNX (Figure 5G) but disturbed the continuity of tissue TNX immunoreactivity along the fetal membranes (Figure 5H). Intracellular TNX staining was

observed in amnion cells supportive of their participation in either synthesis and/or trafficking of AF sTNX.

Discussion

In this study, we identified that TNX, a glycoprotein that interacts with ECM components, was abundantly present in normal AF and its levels decreased as GA advanced. We further observed that women with IAI had significantly increased levels of AF sTNX compared

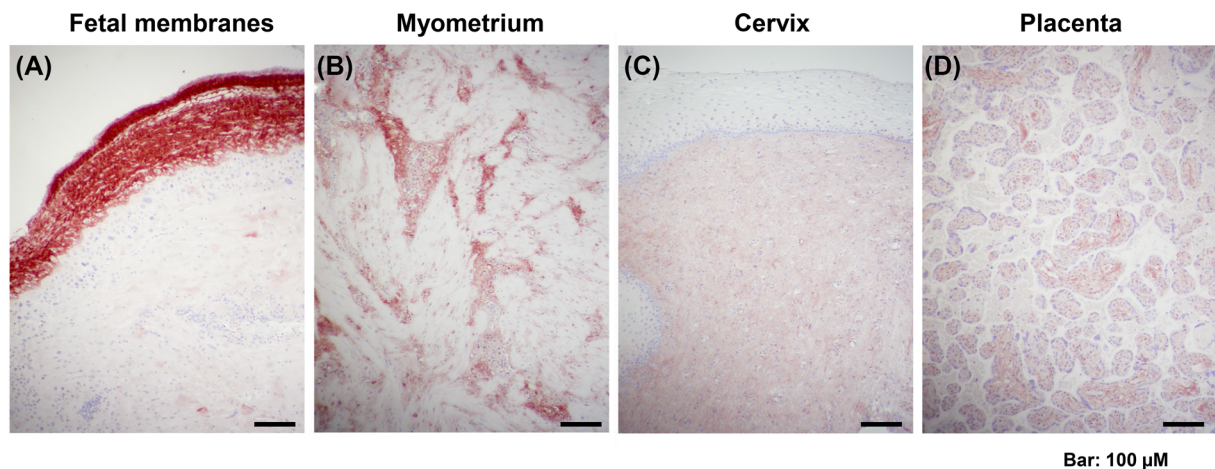


Figure 4. Representative histological images of tenascin-X tissue immunostaining in the human fetal membranes (A), myometrium (B), cervix (C), and placenta (D).

to women without infection and this was independent of membrane status. Conversely, fetal membranes expression levels of TNX were significantly downregulated in women with IAI, and this finding was also independent of fetal membranes' integrity. By using western blotting, we identified that AF of some women with Yes-IAI displays characteristic sTNX proteoforms that are different from those of women without IAI. By immunohistochemistry, we demonstrated that amnion is rich in TNX, but this richness is significantly lost in the setting of IAI. Lastly, fetal membranes consistently displayed a higher level of TNX immunostaining compared to other reproductive tissues.

Tenascins are part of the family of ECM glycoproteins with roles in collagen deposition and assembly, resistance to proteolysis, modulation of collagen stiffness, and cell signaling [35]. The tenascin family includes four members: C, R, W, and X. Tenascin-C is expressed in the developing embryo during skeletal, neural, and vascular morphogenesis, and then virtually disappears in the adult organism. However, in tissues undergoing remodeling processes, tenascin-C is observed during wound repair and neovascularization. Tenascin-R shares a high degree of structural homology with tenascin-C, and its expression appears to be limited exclusively to the central nervous system. Tenascin-W remains the least well-characterized member of the tenascin family with its expression having been found in developing skeletal tissue and neural crest cells, and almost exclusively limited to zebrafish. In contrast, TNX is the first tenascin whose deficiency has been associated with a pathological disorder in humans, a variant of a heritable connective tissue disorder known as EDS, which is associated with fibrillar collagen defects [36].

TNX is the largest known member of the family (~450 kDa) which has been shown to interact with ECM components such as fibrillar (types I, III, and V) and fibril-associated (types XII and XIV) collagens, and the small proteoglycan decorin [37]. The following published experimental evidence lead us to hypothesize that TNX could be involved in PPRM: (1) compared to wild-type fibroblasts, TNX-null fibroblasts display a decreased attachment to fibronectin, which is a key adhesion molecule for fetal membranes [38]; (2) TNX seems to be involved in synthesis and ECM deposition of fibrillar collagens type I, III, and V, which lend tensile strength to the amnion, and whose aberrant gene expression is linked with PPRM [16,39];

(3) the heritable disorder EDS is reported to have an increased risk of PPRM [25].

Collectively, our immunohistochemical, western blot, and RT-PCR data point toward fetal membranes, as a potential source of human AF sTNX. This assertion is supported by previous immunofluorescence experiments which demonstrated that TNX is present in cytoplasmic granules of amnion cells following pharmacologic-induced intracellular accumulation by monensin (disruptor of glycoprotein processing in the Golgi) [40]. At this time we cannot exclude other potential sources, including the fetus, based on prior reports indicating that dermis and blood vessels express TNX during development [41]. However, it is less likely the fetal skin to be the primary source of AF sTNX. It is reasonable to assume that if fetal skin would be the major contributor, the AF sTNX concentration would increase during gestation secondary to increased fetal skin surface during development. The observed GA regulation, with lower AF sTNX levels toward term, is consistent with the clinical observation that 5–10% of pregnancies are complicated by spontaneous rupture of membranes, out of which 60% occur at term [42]. Stretch forces alone cannot be responsible for PPRM. At term, a decrease in the fetal membranes expression level of TNX, indirectly reflected through the AF sTNX levels, could be part of a programed weakening process characterized by onset of cellular apoptosis, increased collagenolytic activity, and collagen remodeling that manifests phenotypically as reduced tensile strength and rupture [5].

In our study, IAI significantly upregulated the levels of AF sTNX and this occurred independent of fetal membranes integrity. The above observation was intriguing because up to this point tenascin-C was believed to be the only tenascin family member that had an inflammatory regulation [43]. Our PCR data demonstrated that expression of *TNXB* mRNA was downregulated in infection. Coupled with the immunohistochemistry data that demonstrated a significant downregulation in immunostaining of the amnion, we propose that the observed upregulation in the AF sTNX levels occurred secondary to the release of TNX from the intra-cellular to the extracellular space. Because in infection amnion cells are damaged, we also propose that the pool of AF sTNX can be enriched secondary to cellular loss and damage. This mechanism would be similar to what was

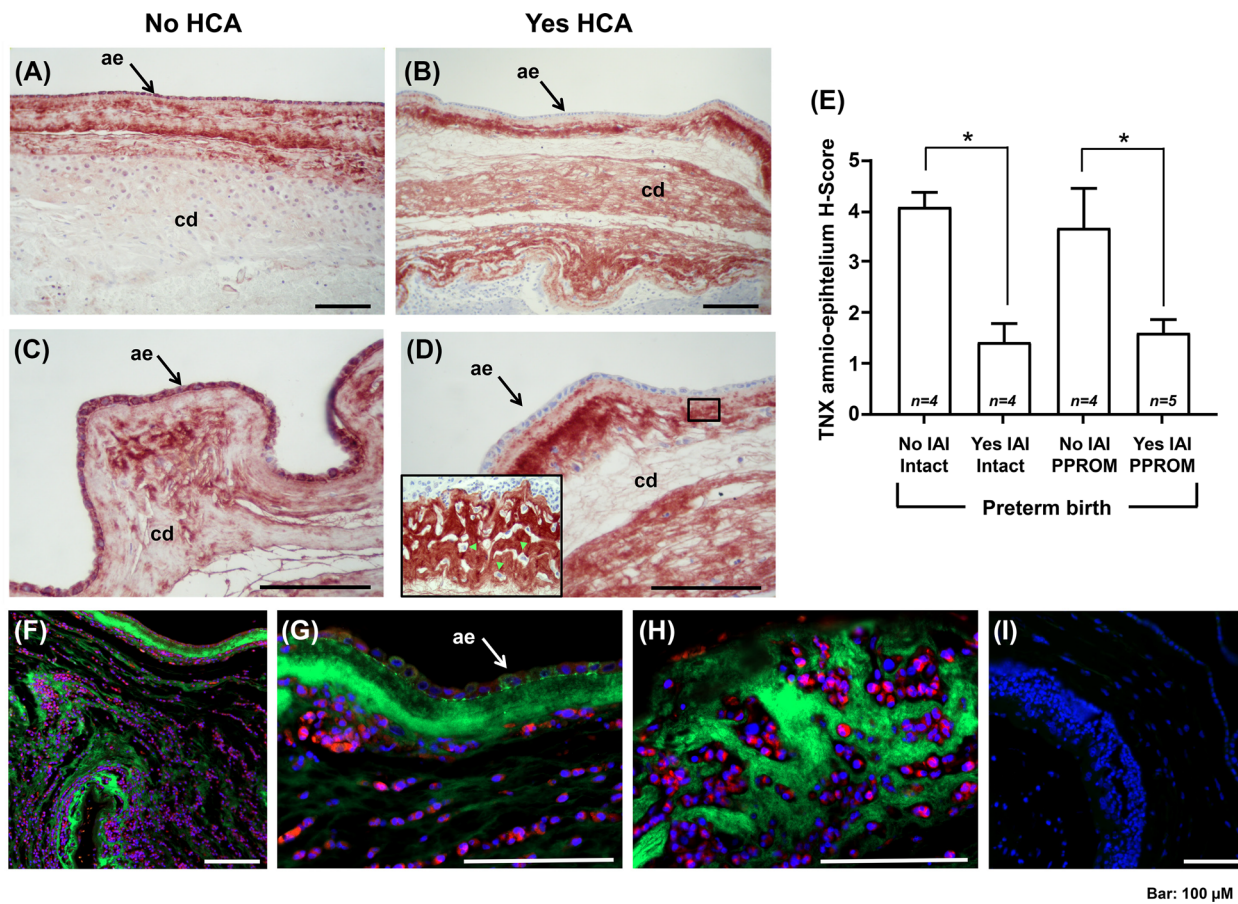


Figure 5. (A, B) Tissue immunostaining of tenascin-X (TNX) in human fetal membranes of women without (No) or with (Yes) histologic chorioamnionitis (HCA). (C, D) The amnio-epithelium (ae, black arrow) and choriodecidua (cd) of women with No HCA display intense staining for TNX, in strong contrast to women with Yes HCA, who exhibited consistently minimal ae staining. At the interface between ae and cd (see insert), the area surrounding the infiltrating inflammatory cells (green fluorescent arrow heads) is clear of TNX. (E) Mean TNX and standard error mean analysis of the intensity of TNX in the ae of women with and without intra-amniotic fluid infection/inflammation (IAI). (F-H) Double immunostaining of fetal membranes for TNX (green fluorescence) and CD45 (red fluorescence) from a representative case with IAI demonstrating presence of tissue infiltrating leukocytes. Nuclei were counterstained with DAPI. The CD45 + inflammatory cells did not express TNX but disturbed the continuity of tissue TNX immunoreactivity along the fetal membranes. Intracellular TNX staining was observed in ae cells (white arrow). (I) Negative control with omitted primary antibodies. * denotes statistical significance at $P < 0.05$.

observed for damage-associated molecular pattern (DAMP) proteins such as high mobility group box 1 (*HMGB1*, previously known as high-mobility group [nonhistone chromosomal] protein 1, high-mobility group box 1) [44]. The DAMP status has not yet been explored for sTNX proteoforms, but was recently demonstrated for tenascin-C which during inflammation elicits activation of innate immune cells via TLR-4 [45].

Similar to our current findings, previous studies have reported multiple species of TNX in human serum, including the ~140 kDa and 75 kDa TNX bands which were previously demonstrated to represent the C-terminal fibrinogen domain of the full-length 450 kDa TNX along with varying number of fibronectin type III repeats [34]. However, lower sTNX molecular forms (~75 kDa) were also identified in human serum, raising the prospect that the collagen fibrillogenesis function of TNX could be exercised through various proteolytic cleavage or alternative splicing variants. In our study, an interesting observation was that the AF of some women with IAI lacked the characteristic 140 kDa band but contained lower molecular weight TNX species. Previous animal studies demonstrated that

the activity of matrix metalloproteinases (MMP)-2 and MMP-9 is significantly higher in *TNX*^{-/-} mice [46]. Based on this evidence we hypothesize that replacement of the predominant 140 kDa TNX form with bands of lower molecular weights reflects proteolysis of TNX secondary to neutrophil activation and MMPs activation [47]. Thus, it is possible that rupture of membranes in women with Yes-IAI and AF with lower molecular weight sTNX species reflects the most advanced stage of collagen disorganization and remodeling that led to PPROM. Our histological observation of a clear halo surrounding the inflammatory cells populating the choriodecidua suggests that proteolysis and clearance of TNX are possible. Future studies are needed to investigate this hypothesis.

Lastly, our study provides a novel comparison among the level of TNX expression in various reproductive tissues. Human fetal membranes seem to express TNX at a significantly higher level compared to myometrium, cervix, and placenta. What can be inferred from our analysis is that TNX may play an important role in maintenance of the integrity of the amnion, which provides strength for the fetal membranes during gestation.

In summary, the herein presented results demonstrate that human AF is rich in sTNX, and the most probable source of this glycoprotein is the amnion. In this study, for the first time we present evidence that inflammation/infection plays a role in the expression of TNX, which is expressed predominantly in the fetal membranes.

Supplementary data

Supplementary data are available at [BIOLRE](#) online.

Supplementary Table S1. Primary antibodies.

Supplementary Table S2. Demographic clinical and outcome characteristics of the women who provided amniotic fluid samples for tenascin-X (n = 334).

Supplementary Figure S1. Flow diagram describing study groups, the number of samples and type of tissues used in this study. Trim, trimester; CRL, control; PTL, preterm labor; PPRM, preterm prelabor rupture of membranes; IAI, intra-amniotic infection/inflammation.

Acknowledgments

We are indebted to the nurses, fellows, and residents at Yale New Haven Hospital, Department of Obstetrics, Gynecology, and Reproductive Sciences and The Ohio State Wexner Medical Center, Department of Obstetrics and Gynecology, and to all patients who participated in the study. Dennis Lewandowski, PhD (affiliation—The Research Institute at Nationwide Children's Hospital) helped with editing and formatting of the manuscript. We thank Dr Mehboob Ali for his assistance with acquisition of the immunofluorescence images.

Authors' contributions

KMR, IAB, and CSB conceived and designed the study, conducted the statistical analyses, drafted the manuscript, had full access to the data in the study, and take responsibility for the integrity of the data and accuracy of the data analysis. All authors acquired and interpreted the data, edited and critically reviewed the manuscript, and approved the final version. IAB and CSB obtained funding.

Role of the funding source

The funding sources had no role in the collection, analysis and interpretation of data; in the writing of the report; and in the decision to submit the article for publication.

Conflict of interests

The authors have no conflicts to declare.

References

1. Maymon E, Chaim W, Sheiner E, Mazor M. A review of randomized clinical trials of antibiotic therapy in preterm premature rupture of the membranes. *Arch Gynecol Obstet* 1998; **261**:173–181.
2. Mercer BM, Lewis R. Preterm labor and preterm premature rupture of the membranes. Diagnosis and management. *Infect Dis Clin North Am* 1997; **11**:177–201.
3. Buhimschi CS, Bhandari V, Hamar BD, Bahtiyar MO, Zhao G, Sfakianaki AK, Pettker CM, Magloire L, Funai E, Norwitz ER, Paidas M, Copel JA, et al. Proteomic profiling of the amniotic fluid to detect inflammation, infection, and neonatal sepsis. *PLoS Med* 2017; **4**:e18.
4. Poletini J, Dutta EH, Behnia F, Saade GR, Torloni MR, Menon R. Aging of intrauterine tissues in spontaneous preterm birth and preterm premature

rupture of the membranes: A systematic review of the literature. *Placenta* 2015; **36**:969–973.

5. Kumar D, Moore RM, Mercer BM, Mansour JM, Redline RW, Moore JJ. The physiology of fetal membrane weakening and rupture: Insights gained from the determination of physical properties revisited. *Placenta* 2016; **42**:59–73.
6. Shook LL, Buhimschi CS, Dulay AT, McCarthy ME, Hardy JT, Duzyj Buniak CM, Zhao G, Buhimschi IA. Calciprotein particles as potential etiologic agents of idiopathic preterm birth. *Sci Transl Med* 2016; **8**:364ra154–364ra154.
7. Lee SY, Buhimschi IA, Dulay AT, Ali UA, Zhao G, Abdel-Razeq SS, Bahtiyar MO, Thung SF, Funai EF, Buhimschi CS. IL-6 trans-signaling system in intra-amniotic inflammation, preterm birth, and preterm premature rupture of the membranes. *J Immunol* 2011; **186**:3226–3236.
8. Anum EA, Hill LD, Pandya A, Strauss JF, 3rd. Connective tissue and related disorders and preterm birth: clues to genes contributing to prematurity. *Placenta* 2009; **30**:207–215.
9. Parry S, Strauss JF, 3rd. Premature rupture of the fetal membranes. *N Engl J Med* 1998; **338**:663–670.
10. Hay ED. Extracellular matrix. *J Cell Biol* 1981; **91**:205s–223s.
11. Menon R, Richardson LS. Preterm prelabor rupture of the membranes: a disease of the fetal membranes. *Semin Perinatol* 2017; **41**:409–419.
12. Bourne GL, Lacy D. Ultra-structure of human amnion and its possible relation to the circulation of amniotic fluid. *Nature* 1960; **186**:952–954.
13. Hampson V, Liu D, Billett E, Kirk S. Amniotic membrane collagen content and type distribution in women with preterm premature rupture of the membranes in pregnancy. *Br J Obstet Gynaecol* 1997; **104**:1087–1091.
14. Strauss JF. Extracellular matrix dynamics and fetal membrane rupture. *Reprod Sci* 2013; **20**:140–153.
15. Chiquet-Ehrismann R, Tucker RP. Tenascins and the importance of adhesion modulation. *Cold Spring Har Perspect Biol* 2011; **3**:a004960.
16. Valcourt U, Alcaraz LB, Exposito JY, Lethias C, Bartholin L. Tenascin-X: Beyond the architectural function. *Cell Adh Migr* 2015; **9**:154–165.
17. Egging DF, van Vlijmen I, Starcher B, Gijzen Y, Zweers MC, Blankevoort L, Bristow J, Schalkwijk J. Dermal connective tissue development in mice: an essential role for tenascin-X. *Cell Tissue Res* 2006; **323**:465–474.
18. Beighton P, De Paepe A, Steinmann B, Tsipouras P, Wenstrup RJ. Ehlers-Danlos syndromes: Revised nosology, Villefranche, 1997. Ehlers-Danlos National Foundation (USA) and Ehlers-Danlos Support Group (UK). *Am J Med Genet* 1998; **77**:31–37.
19. Petersen W, Douglas J. Tenascin-X, collagen, and Ehlers-Danlos syndrome: Tenascin-X gene defects can protect against adverse cardiovascular events. *Med Hypotheses* 2013; **81**:443–447.
20. Czarny-Ratajczak MI, Latos-Bieleńska A. Collagens, the basic proteins of the human body. *J Appl Genet* 2000; **41**:317–330.
21. Bristow J, Carey W, Egging D, Schalkwijk J. Tenascin-X, collagen, elastin, and the Ehlers-Danlos syndrome. *Am J Med Genet C Semin Med Genet* 2005; **139C**:24–30.
22. Christophersen C, Adams JE. Ehlers-Danlos syndrome. *J Hand Surg [Am]* 2014; **39**:2542–2544.
23. Volkov N, Nisenblat V, Ohel G, Gonen R. Ehlers-Danlos syndrome: insights on obstetric aspects. *Obstet Gynecol Surv* 2007; **62**:51–57.
24. Kuczkowski KM. Ehlers-Danlos syndrome in the parturient: an uncommon disorder—common dilemma in the delivery room. *Arch Gynecol Obstet* 2005; **273**:60–62.
25. Barabas AP. Ehlers-Danlos syndrome: associated with prematurity and premature rupture of foetal membranes; possible increase in incidence. *BMJ* 1966; **2**:682–684.
26. American College of Obstetrics and Gynecology Committee Opinion No 161: Method for estimating due date. *Obstet Gynecol* 2014; **124**:863–866.
27. The American College of Obstetricians and Gynecologists, Committee on Practice Bulletins—Obstetrics. Practice bulletin no. 130: Prediction and prevention of preterm birth. *Obstet Gynecol* 2012; **120**:964–973.

28. American College of Obstetricians and Gynecologists' Committee on Practice Bulletins—Obstetrics. Practice bulletin no. 172: Premature rupture of membranes. *Obstet Gynecol* 2016; **128**:e165–e177.
29. Edwards RK, Clark P, Locksmith Gregory J, Duff P. Performance characteristics of putative tests for subclinical chorioamnionitis. *Infect Dis Obstet Gynecol* 2001; **9**:209–214.
30. Salafia CM, Weigl C, Silberman L. The prevalence and distribution of acute placental inflammation in uncomplicated term pregnancies. *Obstet Gynecol* 1989; **73**:383–389.
31. Ghidini A, Salafia CM, Kirn V, Doria V, Spong CY. Biophysical profile in predicting acute ascending infection in preterm rupture of membranes before 32 weeks. *Obstet Gynecol* 2000; **96**:201–206.
32. Dulay AT, Buhimschi CS, Zhao G, Oliver EA, Abdel-Razeq SS, Shook LL, Bahtiyar MO, Buhimschi IA. Amniotic fluid soluble myeloid differentiation-2 (sMD-2) as regulator of intra-amniotic inflammation in infection-induced preterm birth. *Am J Reprod Immunol* 2015; **73**:507–521.
33. Nakano A, Harada T, Morikawa S, Kato Y. Expression of leukocyte common antigen (CD45) on various human leukemia/lymphoma cell lines. *Acta Pathol* 1990; **40**:107–115.
34. Egging DF, Peeters AC, Grebenchtchikov N, Geurts-Moespot A, Sweep CG, den Heijer M, Schalkwijk J. Identification and characterization of multiple species of tenascin-X in human serum. *FEBS J* 2007; **274**:1280–1289.
35. Chiquet-Ehrismann R, Tucker RP. Tenascins and the importance of adhesion modulation. *Cold Spring Harb Perspect Biol* 2011; **3**:a004960–a004960.
36. Burch GH, Gong Y, Liu W, Dettman RW, Curry CJ, Smith L, Miller WL, Bristow J. Tenascin-X deficiency is associated with Ehlers-Danlos syndrome. *Nat Genet* 1997; **17**:104–108.
37. Lethias C, Carisey A, Comte J, Cluzel C, Exposito JY. A model of tenascin-X integration within the collagenous network. *FEBS Lett* 2006; **580**:6281–6285.
38. Minamitani T, Ariga H, Matsumoto K. Adhesive defect in extracellular matrix tenascin-X-null fibroblasts: a possible mechanism of tumor invasion. *Biol Pharm Bull* 2002; **25**:1472–1475.
39. Anum EA, Hill LD, Pandya A, Strauss JF, 3rd. Connective tissue and related disorders and preterm birth: clues to genes contributing to prematurity. *Placenta* 2009; **30**:207–215.
40. Linnala A, Balza E, Zardi L, Virtanen I. Human amnion epithelial cells assemble tenascins and three fibronectin isoforms in the extracellular matrix. *FEBS Lett* 1993; **317**:74–78.
41. Tucker RP, Chiquet-Ehrismann R. The regulation of tenascin expression by tissue microenvironments. *Biochim Biophys Acta* 2009; **1793**:888–892.
42. Duff P, Huff R, Gibbs RS. Management of premature rupture of membranes and unfavorable cervix in term pregnancy. *Obstet Gynecol* 1984; **63**:697–702.
43. Midwood KS, Chiquet M, Tucker RP, Orend G. Tenascin-C at a glance. *J Cell Sci* 2016; **129**:4321–4327.
44. Baumbusch MA, Buhimschi CS, Oliver EA, Zhao G, Thung S, Rood K, Buhimschi IA. High Mobility Group-Box 1 (HMGB1) levels are increased in amniotic fluid of women with intra-amniotic inflammation-determined preterm birth, and the source may be the damaged fetal membranes. *Cytokine* 2016; **81**:82–87.
45. Zuliani-Alvarez L, Marzeda AM, Deligne C, Schwenzer A, McCann FE, Marsden BD, Piccinini AM, Midwood KS. Mapping tenascin-C interaction with toll-like receptor 4 reveals a new subset of endogenous inflammatory triggers. *Nat Commun* 2017; **8**:1595.
46. Matsumoto K, Takayama N, Ohnishi J, Ohnishi E, Shirayoshi Y, Nakatsuji N, Ariga H. Tumour invasion and metastasis are promoted in mice deficient in tenascin-X. *Genes Cells* 2001; **6**:1101–1111.
47. Keelan JA, Yang J, Romero RJ, Chaiworapongsa T, Marvin KW, Sato TA, Mitchell MD. Epithelial cell-derived neutrophil-activating peptide-78 is present in fetal membranes and amniotic fluid at increased concentrations with intra-amniotic infection and preterm delivery. *Biol Reprod* 2004; **70**:253–259.